Estimation of elevated black carbon episode over Ukraine using Enviro-HIRLAM

Mykhailo Savenets[1], Larysa Pysarenko[1], Svitlana Krakovska[1], Alexander Mahura[2] and Tuukka Petäjä[2]

[1]Ukrainian Hydrometeorological Institute (UHMI), Kyiv, 03028, Ukraine

[2]Institute for Atmospheric and Earth System Research (INAR), Faculty of Science, Physics / University of Helsinki (UHEL), Helsinki, 00560, Finland

Correspondence to: Mykhailo Savenets (savenets@uhmi.org.ua), Alexander Mahura (alexander.mahura@helsinki.fi)

Abstract. Biomass burning is one of the biggest sources of black carbon (BC) concentrations which negatively impacts human health and contribute to climate forcing. In this work we explore horizontal and vertical variability of ~~black carbon~~BC concentrations over Ukraine during a wildfire episode in August 2010. Using Enviro-HIRLAM modelling framework the ~~black carbon~~BC atmospheric transport was modelled for coarse, ~~and~~ accumulation and Aitken mode aerosol particles emitted by the wildfire. Elevated pollution levels were observed within the boundary layer. The influence of the ~~black carbon~~ BC emissions by the wildfire was identified up to 550 hPa level for the coarse and accumulation mode and at distances of about 2000 km from the fire areas. ~~Strong temperature inversions at nighttime resulted in subsiding air mass movement and lead to increased concentrations of black carbon in the atmospheric boundary layer.~~ As modelling is the only available source of BC data in Ukraine, our results were compared with ~~G~~ground-based measurements of dust, which showed ~~of dust showed~~ increase of concentration up to 73% in comparison to average values. BC contribution was found to be 10-20% among total aerosol compounds near the wildfires in the lower 2-km layer. At the distance, BC exceeded 10% only over the urban areas. In the areas with high BC content represented by both accumulation and coarse mode, downwelling surface long-wave radiation increased up to 20 W/m^2 and 2-m air temperature increased on 1-4°C during the midday hours. ~~The fingerprint of local fires was found in the areas with local maxima of summary black carbon values for coarse mode.~~ The findings of the case study could help to understand the behaviour of ~~black carbon~~BC distribution and possible direct aerosol effects during anticyclonic conditions which often observed in mid-latitudes in the summer and lead to wildfires occurrence.

1 Introduction

Black carbon (BC) is the component of fine particulate matter (PM$_{2.5}$) considered as one of the contributors to climate forcing next to carbon dioxide (Bond et al., 2013, Kurganskiy et al., 2015) and highly probable harmful health impact (Janssen et al., 2011; WHO, 2012; O'Dell et al., 2020). BC is formed as a product after incomplete combustion of biomass and fossil fuels (e.g., Forbes et al, 2006, Bond et al., 2013). Large amount of BC is emitted into the atmosphere from biomass burning (Konovalov et al., 2018) as a part of total chemical species flux during wildfires (Amiro et al., 2001; Barnaba et al., 2011; Virkkula et al. 2014a), which cause elevated pollution levels around burned areas (e.g., Virkkula et al. 2014b; Wu et al., 2018;

Castagna et al., 2021). BC content and different aerosol constituents in case of huge emission frequently estimated by using atmospheric modelling (Hodzic et al., 2007; Bessagnet et al., 2008; Konovalov et al., 2018; Singh et al., 2018; Magalhaes et al., 2019; Kostrykin et al., 2021) and sometimes in-situ measurements (Yttri et al., 2007; Eleftheriadis et al., 2009; Singh et al., 2018; Jia et al., 2021). In contrast to other the aerosol compounds, BC typically cause radiative a positive forcing (Bond et al., 2013; Stjern et al., 2017) which intensity depends on the particle size (Matsui et al., 2018). Consequently, the heating effect is generally observed from wildfire emissions (Kostrykin et al., 2021), and also from anthropogenic sources (Zhuang et al., 2019). Sometimes a cooling effect was also detected (Ma et al., 2018). All these effects, however, are localized (Modak and Bala, 2019). In Ukraine, there are no observations for carbonaceous aerosols in the atmosphere. Moreover, only few studies have mentioned about Ukrainian territory and BC distribution during wildfire events (Pavese et al., 2002; Yang et al., 2017).

As a starting point for the current case study, the forest fire events occurred in summer 2010 at the centre of the European territory of Russia with strong wildfire emissions. These emissions supported by extremely hot weather and rainless conditions. Several studies discussed different aspects of this event, including aerosol distribution (Galytska et al., 2010; Konovalov et al., 2011; Witte et al., 2011; Galytska et al., 2016), radiative effects (Chubarova et al., 2012) and air temperature changes (Pere et al., 2014). The emissions were detected and influenced atmospheric composition in Finland as well (Leino et al., 2014). The most severe period was connected withrelated to the August fires with a lot of pollution transported towards Ukraine (Galytska et al., 2016) and it ended after 18th August when the pollution levels returned to typical for these geographical regions (Witte et al., 2011).

In more detail, Galytska et al. (2018) focused on analysis of summer 2010 wildfires' events and on studying aerosol content changes for period 1 July – 20 August 2010. This study used satellite data from the Moderate Resolution Imaging Spectrometer (MODIS) and the Cloud-Aerosol Lidar with Orthogonal Polarization (CALIOP) for detecting burned areas, aerosols' vertical profiles and clouds. Data from ground-based sun photometers of Aerosol Robotic NETwork (AERONET), measuring column-integrated aerosol optical depth (AOD), were validated against the satellite measurements. The Hybrid Single-Particle Lagrangian Integrated Trajectory (HYSPLIT) model was used to simulate air mass backward trajectories (with vertical levels of 0.5, 1.5, 3, 4 and 5 km), and analysis of meteorological situation and air masses transport were performed with help of a series of synoptic maps. The maximum AOD above Moscow (Russia) on 7th August was associated with airflows from the central part of Russia at levels of 0.5–1.5 km passing through fire areas. In Kyiv, the maximum AOD was registered on 15th August (up to 4 km level) with air movements from the forest fire regions. The simulated air trajectories referred to anticyclonic movements in both cases. These conditions facilitated stagnation of air and accumulation of pollutants in the region of interest. In Sevastopol, the maximum AOD was observed on 16th August within the layer 0.5–5 km due to air masses transport from the territory of active fires.

Spatiotemporal distribution of trace gases and aerosol at the ground level was analysed by Konovalov et al. 2011. The total
CO, PM_{10} and O_3 concentrations were analysed using satellite measurements and the CHIMERE chemistry transport model
(Konovalov et al., 2011) with the most attention to the Moscow region. It was found that extremely high levels of daily mean
CO and PM_{10} concentrations reached 10 and 700 μg/m³ respectively. O_3 concentrations were episodically very large (up to
400 μg/m³) even after emission significantly decreased. It was estimated that approximately 10 Tg CO were emitted in the
Moscow region during the 2010 heat wave (more than 85% of the total annual anthropogenic CO emissions). Aerosol, emitted
from summer 2010 wildfires caused shortwave direct radiative effects (Pere et al., 2014). Significant reduction of diurnal
average solar radiation was found to be at the ground and up to 80–150W/m². The resulting feedbacks lead to a cooling of the
air up to 1.6°C at the surface and up to 0.1°C at altitudes of 1.5–2.0 km.

Described wildfire events frequently occur in Ukraine or in territories of neighboring countries that develop into elevated
pollution events. Unfortunately, the existing official Ukrainian air quality monitoring network (UA-AQMN) does not provide
any measurements of BC. Hence, the modelling remains the only possible way to estimate the spatio-temporal variability of
BC in Ukraine, and to explore the consequences of elevated pollution episodes and assess the short-term impacts in the region.
The lack of observation capacity on BC on a national level caused a gap in knowledge on how BC is distributed; what are the
impacts on local ecosystems; and which mitigation measures are needed to improve the situation. This study is the first in
Ukraine which describes the elevated spatio-temporal BC content on the three-dimensional scale, explores the distribution of
BC in particle sizes and compares the BC ratio between other aerosol components in the atmosphere with the emphasize on
extremely hot weather episodes. Furthermore, we aimed to estimate the impact of wildfire emissions on the surface by
considering direct aerosol effects, as the response of radiative and temperature regimes varying in different regions and
depending on the ratio of aerosol components.

We explored the BC concentrations in Ukraine during the intensive biomass burning episodes in the region in August 2010.
We deployed Environment – High Resolution Limited Area Model (Enviro-HIRLAM) modelling system in the analysis. It is
a fully online coupled (integrated) numerical weather prediction (NWP) and atmospheric chemical transport (ACT) modelling
system for research and forecasting of meteorological, chemical and biological weather (Baklanov et al., 2017). These
simulations will help us to understand temporal and spatial BC distribution after wildfire emissions in case of summer
anticyclonic conditions leading to frequent wildfires occurrence in mid-latitudes and resulted elevated pollution levels. Here
we initialized a case study was carried out for elevated pollution episodes in August 2010 over Ukrainian territory caused by
atmospheric pollution transport from the severe forest fires occurred in central part of Russia. BC concentration and its
distribution were estimated for extended period 2-18 August 2010 considering the extreme pollution episode lasted 7-17
August 2010. Direct aerosol effects on downwelling surface short-wave/ long-wave radiation and 2-m air temperature also are
discussed. Analyses were conducted for both the accumulation and coarse modes as their particle sizes tend to collect in the
lowest atmospheric layers and mostly could have influence on human health.

2 Data and methods

2.1 Enviro-HIRLAM setup

100 The Enviro-HIRLAM system consists of two main blocks. The HIRLAM model itself as ~~a~~an NWP model, which could be used for research and operational purposes (HIRLAM-5 Scientific Documentation, 2002). The Enviro-components are integrated into the NWP model (Baklanov et al., 2017). These components include a variety of atmospheric chemistry schemes, which simulate tropospheric sulphur cycle chemistry, gas-phase chemistry, photolysis rates, heterogeneous chemistry, aerosol formation and dynamics, its wet and dry deposition, different feedback mechanisms (direct, semi-direct, indirect). For

105 modelling of fluxes of BC, the Enviro-HIRLAM has been already used for the Northern Europe and Arctic regions (Kurganskiy et al., 2015; Nuterman et al., 2015).

The model domain for runs covers almost all the European territory and ~~it~~ is enlarged for considering the atmospheric circulation in the middle latitudes. It consists of 500x400 grids along longitude vs. latitude. It has 15-km horizontal resolution

110 and time step of 120 sec. The area of interest is within 20–45°E and 40–60°N (Fig. 1). Generated model output is saved at every 3 h interval.
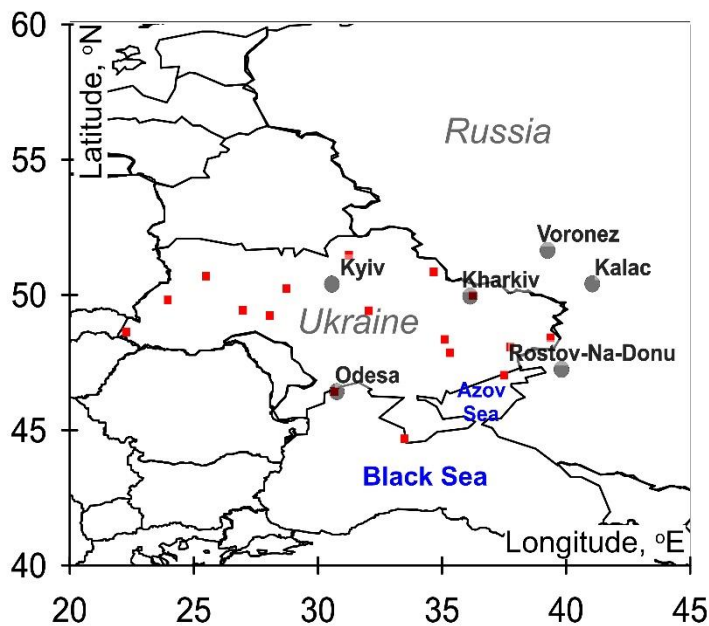
Figure 1: The area of interest and locations (black dots) of the radiosoundings stations (Kyiv, Odesa, Kharkiv, Voronezh, Rostov-na-Donu, Kalac) and locations (red squares) of air pollution monitoring stations used in this study.

115

The vertical structure includes 40 model levels (up to 10 hPa) with more detailed resolution in the boundary layer. In general, main weather-forming layer (i.e., up to 500 hPa) includes 22 model levels. This provides a great opportunity for studying the BC vertical atmospheric transport. The model was run as the following: at first, the reference (or control) run (REF) and then, the run with direct aerosol effects (DAE) included. However, for the purpose of the BC spatio-temporal analysis during severe
120 forest fire episode (7-17 August 2010) we decided to use the output of only a reference run.

The initial and boundary conditions (ICs/BCs) for meteorology include components of winds speed, air temperature and specific humidity extracted at all model levels and at every 3-hour interval from ERA5 model archives at the European Centre for Medium-Range Weather Forecasts (ECMWF). The sea surface temperature and the conventional BUFR (The Binary
125 Universal Form for the Representation of meteorological data) observations (for data assimilation) were extracted at every 12-hour and 3-hour interval, respectively. The ICs/BCs for gas and aerosol concentrations included 3D fields of mixing ratio of aerosol components (dust, hydrophilic and hydrophobic organic matter and black carbon, sulphates) as well as gases (O_3, SO_2, NO_2, NO, hydrogen peroxide (H_2O_2), hydroxyl radical (OH), nitrate radical (NO_3), hydroperoxyl radical (HO_2), dimethyl sulfide (DMS)) were extracted at all model levels and at every 3-hour interval from Copernicus Atmosphere Monitoring
130 Service (CAMS) of ECWMF.

A suite of emission inventories (EIs) was utilized in the model runs, including anthropogenic and biomass burning (wildfires). In more detail, the EIs (given in geographical latitude/longitude domain) – for the global biomass burning (wildfires) emissions (IS4FIRES; Sofiev et al., 2012), Evaluating the Climate and Air Quality Impacts of Short-Lived Pollutants (IIASA's ECLIPSE,
135 5th version) (gridded emissions of gases and aerosols of SO_2, NO_x, NH_3, nmVOC, BC, OC, $PM_{2.5}$, PM_{10}, CO, CH_4 for SNAP codes (Selected Nomenclature for Air Pollution) such as industry, transportation, agriculture, etc.), shipping emissions (include SO_2, BC and OC), emissions of DMS (Nightingale et al., 2000). The mission preprocessor includes both vertical and temporal profiles for the model setup.

140 The spatial analysis of modelling results model output was carried out considering all grid cells without spatial averaging and interpolation. It allowed detecting concentrations changes within each grid caused by anticyclonic air movements. Evaluation of accumulated BC impact was performed by time integration of concentration for studied period. Therefore, the summed values represent the total amount (for both the Aitken, accumulation, and coarse modes) transported by air movements through grid cells.

145 **2.2 Additional data for analysis**

Unfortunately, UA-AQMN does not provide measurements of BC, moreover PM also is not measured. Dust – is the only available pollutant which could be compared to the modelled aerosol species. The dust is measured at more than120 monitoring

sites, and measurements contain all coarse aerosol particles regardless of their origin (Nadtochii et al., 2019). Dust concentration on these sites is measured using the method of weighing the total suspended particles (RD, 1991).

150 -Therefore, it is complex to compare accurately results with ground-based measurements. UA-AQMN was established several decades ago, and under continuous development and expansion. Therefore, majority of the monitoring sites are situated in cities. Such cities have large number of anthropogenic sources such as factories, thermal power stations, roads, etc. Hence, it is reasonable to use daily averaging and to calculate integral value for each city based on several monitoring stations. Such approach can improve signal-to-noise ratio in a time series. In our study, dust mass concentration data was selected from year

155 2010 in 20 Ukrainian cities, which are approximately geographically equally distributed within the country. It was done for purposes of intercomparison between western-eastern-southern-northern territories.

The upper air soundings data from the Wyoming University database (http://weather.uwyo.edu/upperair/sounding.html) were used to detect temperature inversions. The air temperature vertical profiles were analyzed for 2–18 August 2010 at the

160 following soundings stations: Kyiv (station code 33345), Kharkiv (34300), Odesa (33837), Rostov-na-Donu (34731), Kalac (34247) and Voronezh (34122). Voronezh and Kalac are situated near the areas where the forest fires occurred. Kharkiv and Rostov-na-Donu were selected for estimation of inversion impact at some distance from the fires. Kyiv and Odesa were chosen as relatively distant to sources of the emissions. The temperature vertical profiles were taken into consideration up to 3–3.5 km above the ground surface at 00 UTC times during the studied period.

165 **3 Results and discussion**

3.1 Synoptic weather situation and the dispersion of wildfire emissions during summer August 2010 in Ukraine

According to the Climate Forecast System (CFS) Reanalysis (source: www.wetterzentrale.de) of the 500 hPa geopotential maps over Europe, the blocking anticyclone, which caused severe hot weather, lack of precipitation and occurrence of wildfires, lasted from the end of June to the second half of August 2010 over the East Europe and south-western regions of

170 Russia (see example Fig. A1Fig. 2). Hot air masses from Central Asia penetrated into the north-west, and anticyclone was detected throughout the whole troposphere before the highest pollution levels distributed out of burning cells. Continuous extreme weather and clear sky conditions together with highest insolation in the middle latitudes caused domination of high temperature and low humidity regimes. These were the most favorablefavourable conditions for drought formation that played crucial role in emerging fires and their rapid distribution.

175

At the beginning of August 2010 before the wildfire episode, the BC content over Ukraine was low and mostly it was represented by the accumulation mode with the values of 1-8 ppb. The highest BC concentrations reached 16 ppb

180

The main source of wildfire emissions was located outside of the Ukraine's territory and consisted of several burning areas (see Fig. 2b). Observed anticyclonic conditions influenced on formation and development of spatio-temporal patterns for BC atmospheric transport and dispersion. The time-series for each grid point consist of two maxima. These ~~are connected with~~relate to observed dominated atmospheric circulation patterns. Typical clockwise air movement for anticyclones in the Northern Hemisphere caused intensive atmospheric transport towards Ukraine during two episodes: 7-8 and 13-16 August 2010. For these episodes, elevated concentrations were also observed in the northern regions of Ukraine (as shown in Fig. 2).
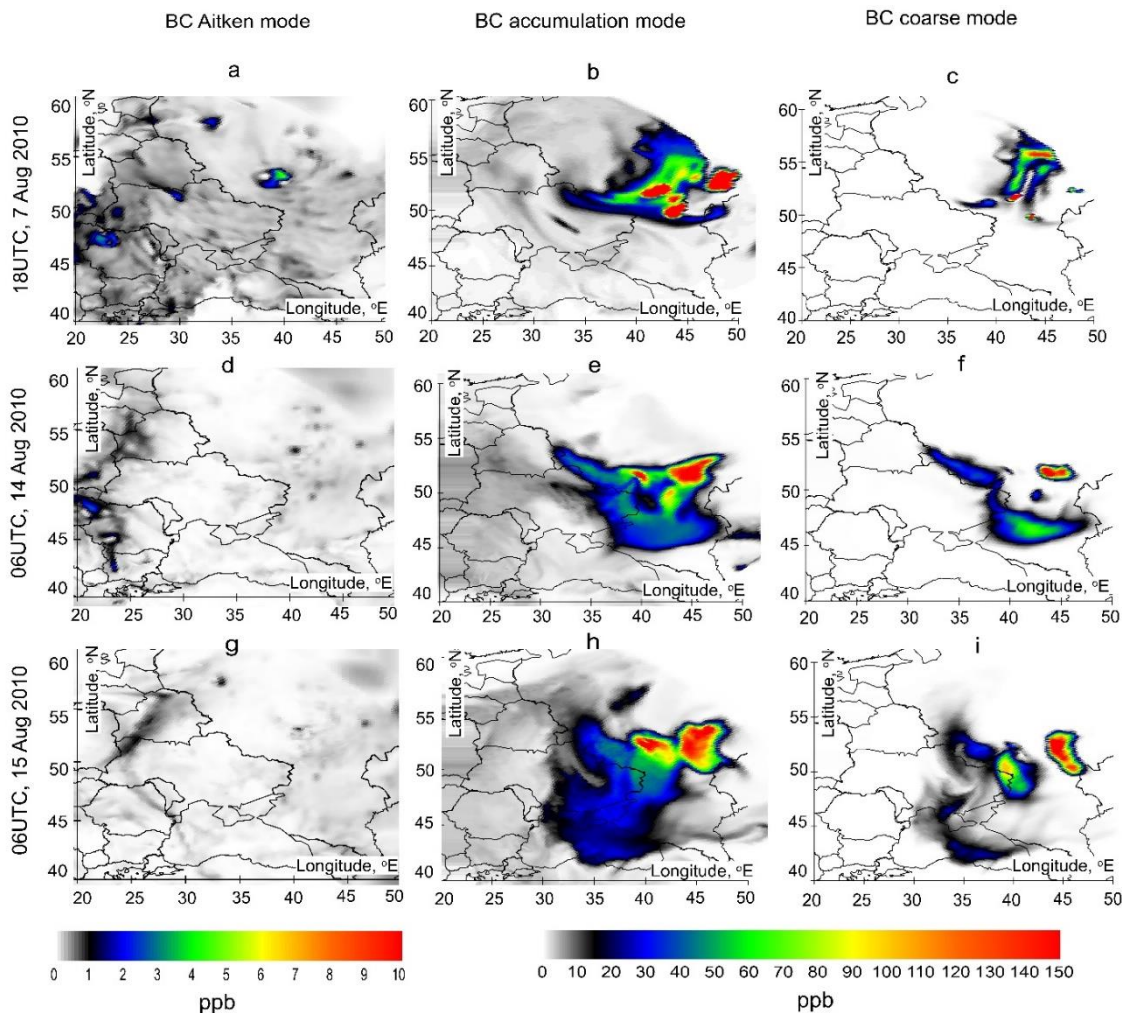
Figure 2: The spatial distribution of the BC for the Aitken (a,d,g), accumulation (b,e,h) and coarse mode (c,f,i) during the episodes of its highest concentrations at the near-surface level in the days of air movement towards Ukraine.

For those days the highest values for BC (accumulation mode) in the boundary layer exceeded 400-600 ppb near the burning cells and 70-150 ppb over the selected territories of eastern, central and northern parts of Ukraine. For coarse mode, these values were 300-450 ppb and 20-60 ppb for the same territories, respectively. The highest values for BC Aitken mode did not exceed 6 ppb near the fires and the simulated values were lower than 2 ppb at distances from the burning areas. Moreover, the

195 highest values of Aitken mode were intermittently observed over urban areas reaching 10 ppb. Due to burning cell's location, maxima in time series shifted from the east and north-east to the west and south-west regions of Ukraine. The shifting period depended on anticyclonic air masses movement. Nevertheless, during 7–8 and 13–16 August, the higher values in the western part of Ukraine were observed within 24 h after maxima emerged on the east. During ~~unfavorable~~unfavourable circulation conditions, the BC plumes were transported and dispersed at distances more than 2000 km away from the original burned

200 areas. The dominated hot and dry weather conditions interrupted in the second half of August 2010. It occurred when blocking anticyclone weakened and cyclone arrived from the western sector.

In general, the wildfire emissions have a large accumulative effect in the near-surface layer. Total accumulated amount of BC for the period 3–18 August 2010 reached 13500 ppb (for the accumulation mode) and 2200 ppb (for the coarse mode) in the

205 lower tropospheric layer near the burning areas (Fig. 3). The total accumulated amount of BC Aitken mode caused by wildfires was about 15-30 ppb, whereas the maximum accumulated impacts were observed in the cities (see e.g., Aitken mode on Fig. 3). A large amount of combustion products was transported through the atmosphere to the south-west and deposited over the territories of the Eastern Ukraine, the Azov and Black Seas. The integral values of BC on these territories exceeded values of 800 and 150 ppb for the accumulation and for the coarse modes, respectively. This is well seen in Fig. 3 where the regions

210 were affected by intensive deposition processes. Due to the smaller sizes of the particles, the accumulation mode had a larger spatial extent and more smooth distribution than the coarse mode.
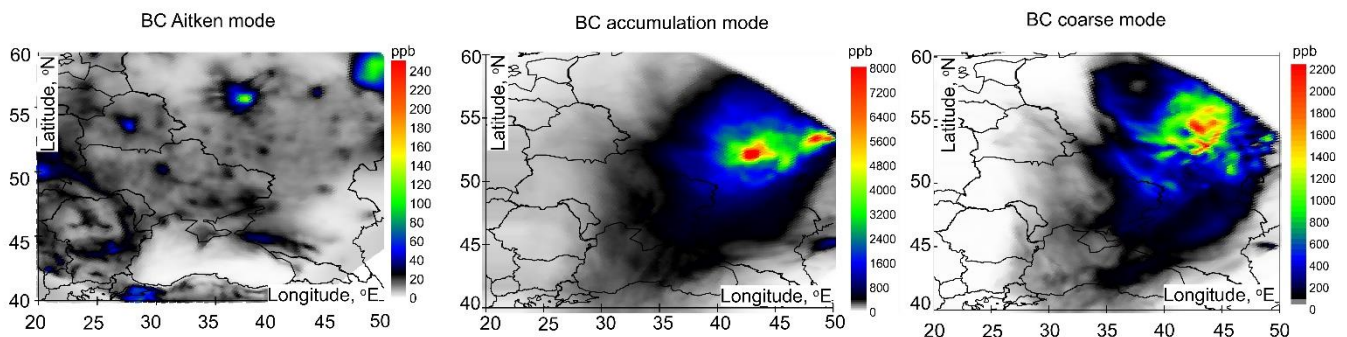
Figure 3: The integral value of the near-surface BC concentrations for the Aitken, accumulation and coarse modes for the period 3-18 August 2010.

For the studied period, in general, the ground-based dust measurements also showed elevated levels connected with the forest fires. Almost all the geographical regions except northern part of Ukraine experienced a clear maxima of ground-based dust concentrations during August 2010. The highest exceeding over the urban background values in August were observed on the eastern territories. In this case, the integral value of the near-surface BC concentrations for the coarse mode was higher than 250 ppb. For the cities on the east, the dust concentrations were 27–47% higher than the average dust content in 2010. Moreover, these values were also 23–72% higher than multi-year average concentrations for the month of August. Overall, the dust content on the east Ukraine was 0.02–0.07 μg/m^3, which was higher than usually occurred in August.

Large difference in the dust content between August and other months was observed on the seashore of the Azov Sea and in the central part of Ukraine. The concentrations were higher by 0.05–0.25 μg/m^3 than usually in the same month. A majority of cities in the central part of Ukraine showed 17–73% higher dust concentrations than average in 2010 and concurrently 8–45% higher than usually in August. In the western parts of Ukraine, the integral values were lower than 100 and 500 ppb for coarse and accumulation modes, respectively (Fig. 3).

3.~~3~~ 2 Diurnal variability and vertical distribution of BC in the region

During 3-18 August at ~~nighttimes~~night times the whole European territory of Russia, central and eastern territories of Ukraine were characterized by presence of surface air temperature inversions. Therefore, it is well seen through BC diurnal variations in the lowest 500-meter layer. The deepest and strongest (up to 655 m depth and up to 12.5°C) inversions were observed during 4–7 and on 16 August (see Fig. ~~3~~A2). At 500 m level the air temperature was warmer by 10–12°C than at 2 m. For other nights the inversions were weaker with an average difference of 3–4°C in the 2-500 m layer.

In our study, diurnal variations of BC content in the boundary layer were well detected. Maxima more often ~~were~~was observed at night and morning hours, whereas daytime pollution levels in the lower troposphere were low. These diurnal variations appeared due to radiative surface cooling on summer nights, and especially in case of blocking anticyclones. Such anticyclones cause forming of air temperature surface inversions. Together with intensification of downward air movement at nighttimes, BC from the whole lower and middle tropospheric levels is accumulated within the boundary layer reaching elevated values there. During daytime, the processes of less intensive air descending and turbulence increasing are resulted in more homogeneous vertical distribution. Hence, it can lead to decrease of near-surface BC content. As it happened throughout the Ukraine's territory with anticyclonic weather, BC spatial distribution at the separate level in the lower troposphere looks more with dominating horizontal dispersion. This may cause confusion about physical reasons of observed diurnal changes. In the middle troposphere any diurnal variations of BC content are negligible because surface inversions do not reach these altitudes. The vertical distribution of BC coarse and accumulation mode ~~particles~~ was well detected in the lowest 3-km layer with the maximum observed in the boundary layer. Approximately at 700 hPa level, BC concentration for both accumulation and coarse

modes started to decrease very rapidly (Fig. 4). The levels of 660-630 hPa for the coarse mode and 620-590 hPa for the
250 accumulation mode were identified as the highest altitudes where the influence of wildfire emissions was detected constantly
during daytime. Rarely, ~~during the midday~~ elevated BC concentrations were detected at 590 hPa (for the coarse mode) and at
550 hPa (for the accumulation mode) with the concentrations lower 0.1 ppb.

In contrast to the BC coarse and accumulation modes, Aitken mode was observed throughout the entire troposphere up to 200
255 hPa level (Fig. 4) height, however the wildfire emissions did not prevail over the anthropogenic emissions. The BC Aitken
mode rarely exceeded 0.2 ppb at 950 hPa level. Therefore, concentrations more than 1 ppb were observed only near the surface
and had clear maximum over urban areas (see Fig. 3). This is the reason why the BC Aitken mode near the surface was higher
in more distant Odesa than in Kalac region.
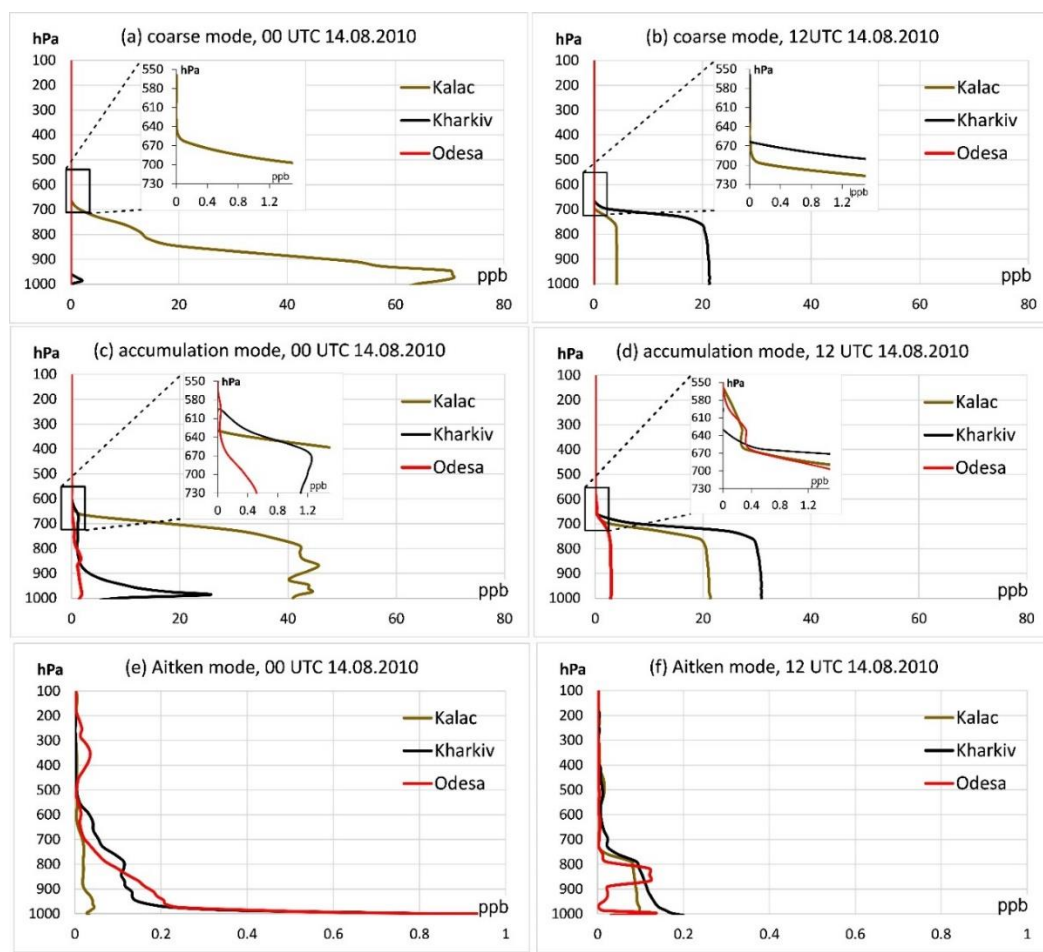
260

Figure 4: BC vertical profiles for coarse (a,b), accumulation (c,d) and Aitken (e,f) modes over Kalac, Kharkiv and
Odesa at 00UTC (a,c) and 12UTC (b,d) on 14th August.

It is well seen from the Fig. 4 that BC rather equally distributed in the 1000–700 hPa layer during day hours. But at nightime, BC was observed mostly in the boundary layer, especially the coarse mode. Temperature inversions and air descending during night hours caused more intense coarse mode deposition, therefore it is hard to find coarse particles at the distance more than 1000 km out from the active fires (represented by Odesa on Fig. 4). However, accumulation mode could be transported at such long distances and the transportation was observed at the lower 3-km layer.

~~3.4 Spatial variability in BC in Ukraine during the wildfire episode~~
3.3 Ratio of aerosol compounds and observed direct aerosol effects during the wildfire episode

Aerosol impacts on the atmospheric composition during wildfire events depend on the intensity of the fire (Vadrevu et al., 2015), on the fuel (Christian et al., 2003; Lee et al., 2018) and the stage of the fire (e.g., open fire, smoldering fire (Lee et al., 2010; Popovicheva et al., 2019)). These features will influence for example the ratio of CO/CO_2, amount of black carbon emissions as well as the vertical distribution of BC. Enviro-HIRLAM simulations were conducted considering five main aerosol compounds: BC, organic carbon, sulfate, sea salt and mineral dust. The highest values of BC-to-total aerosol content ratio observed in the lower 200-m layer (up to 990 hPa) over fire areas reaching 20% (see Fig.5a). BC normally accounts for 10% at the distance from wildfires by the prevailing wind (Fig. 5d-5i). On the example of Odesa (the most distant city among presented), it is well seen the influence of local urban BC emissions, where BC ratio increased to 15-24% near the surface (see Fig. 5j-5l). Vertical distribution of BC ratio was rather uniform from the surface to the altitude of 2 km (≈800 hPa).
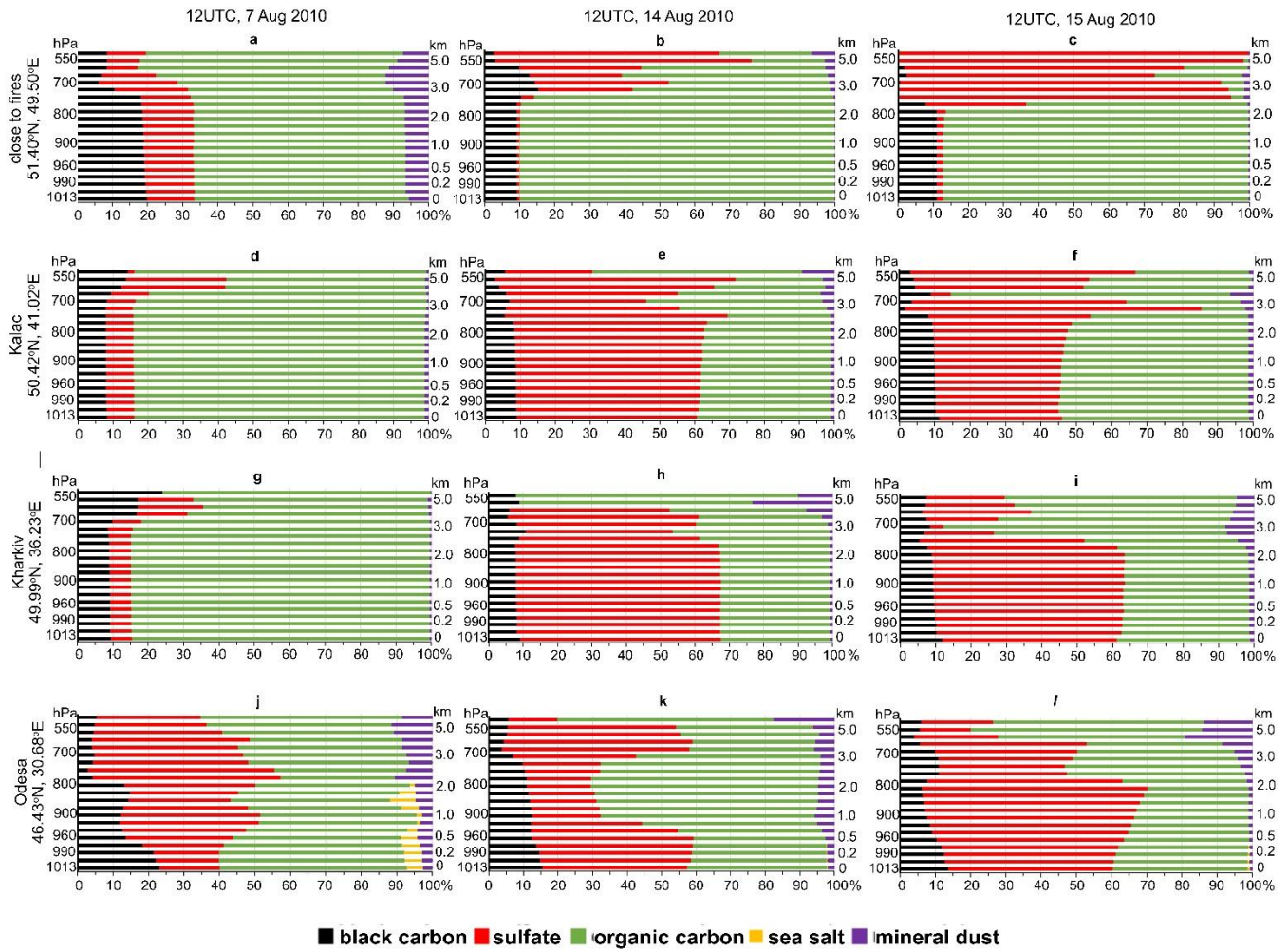
Figure 5: Vertical distribution of ratio of aerosol compounds in the days of air movement towards Ukraine at 12UTC on 7th August (a,d,g,j), 14th August (b,e,h,k) and 15th August (c,f,I,l).

Organic carbon very often is the main aerosol component in the lower 2-5-km layer (≈800-550 hPa), especially near the fires, but also at the surface in general (e.g., Jimenez et al. 2009). Based on our results, sulfates prevail throughout the lower and middle troposphere at the distances, and over 3 km (≈700 hPa) level near the wildfires. Hence, aerosol effects over the region were mainly driven by organic carbon and sulfate aerosols. The largest BC contribution during anticyclonic weather conditions seem to be in the boundary layer. In our analysis, mineral dust ratio rarely exceeded 10%, whereas sea salt was detected in the atmosphere only near the sea (see Fig. 5j, 5l).

Based our modelling results, continuous wildfires and aerosol emissions over the region as a consequence influenced the radiative transfer via direct aerosol effects. Enviro-HIRLAM DAE run showed both increase and decrease of downwelling

295 surface long-wave and short-wave radiation. The most intense changes caused by direct aerosol effects were observed during the midday reaching over ±20 W/m² for long-wave and over ±100 W/m² for short-wave radiation (see example on Fig. 6). The observed direct effects on the downwelling surface radiation co-aligned with the total aerosol impact. Our results indicate that when the BC concentration and the coarse mode exceeded 30 ppb and BC-to-total aerosol mass ratio was over 10% in the lower troposphere, the downwelling surface long-wave radiation tended to increase while the changes of short-wave radiation

300 varied within -200…25 W/m².
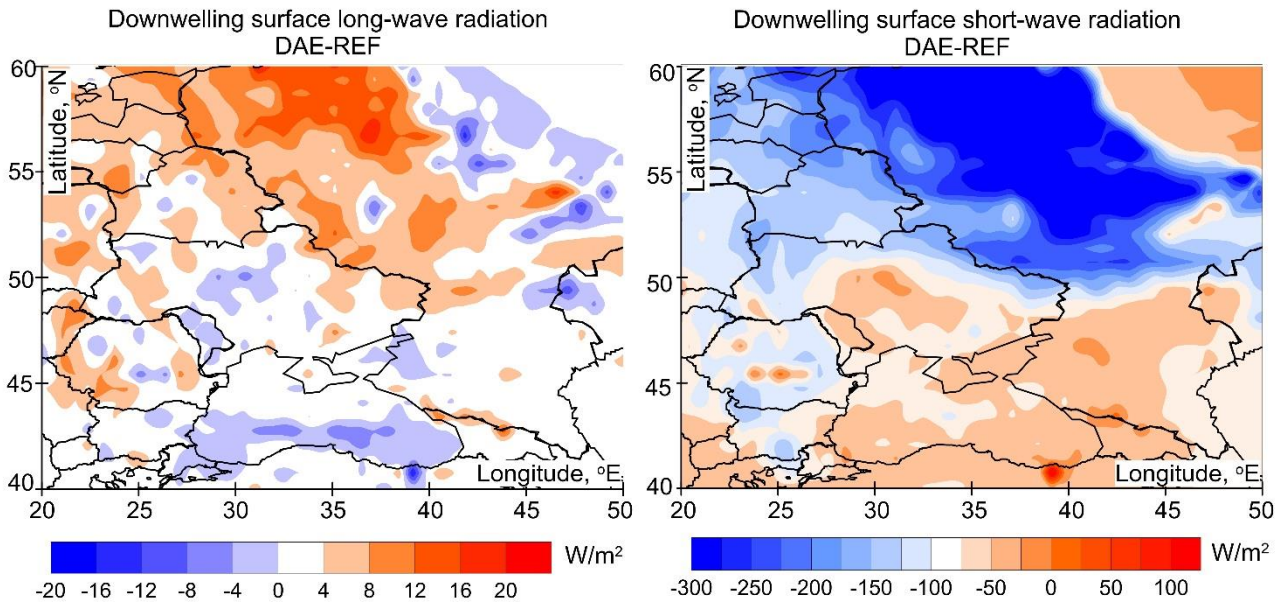
Figure 6: Differences between DAE and REF for downwelling surface long-wave and short-wave radiation at 12UTC on 14th August 2010.

305

In our simulations, direct aerosol effects had an impact on temperature as well. The difference between DAE and REF runs showed that 2-m air temperature during the midday varied from -3°C to 3°C (see Fig. 7). The 2-m air temperature decreased due to the direct aerosol effects prevailed during the wildfire episode. However, the 2-m air temperature was higher with direct aerosol effects in areas where DAE downwelling surface long-wave radiation was higher 12 W/m² and DAE-REF difference

310 for surface short-wave radiation was not lover than -150 W/m². Moreover, the 2-m air temperature was 1-4°C higher at the distance from the wildfires over the territories where the BC coarse mode exceeded mixing ratios of 20-30 ppb.
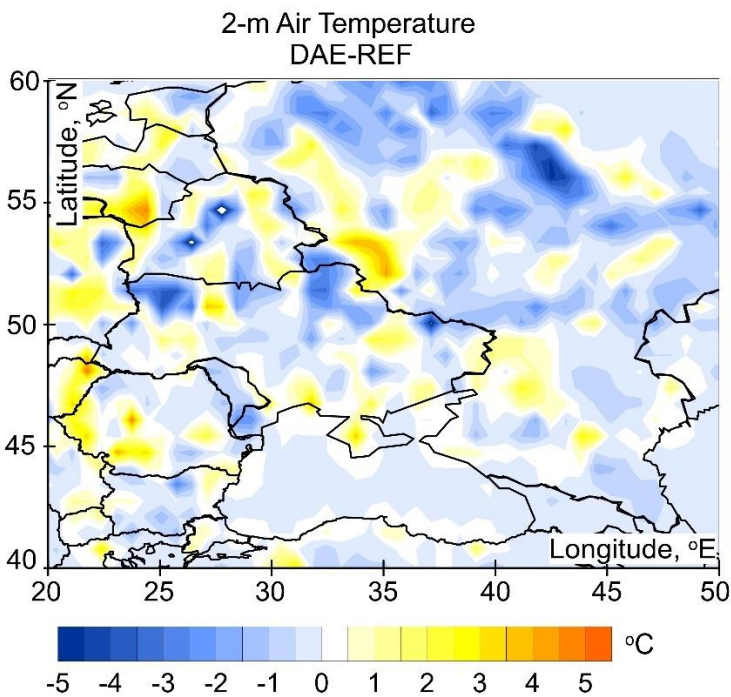
Figure 7: Differences between DAE and REF for 2-m Air Temperature at 12UTC on 14th August 2010.

315

3.4 Discussion

The BC dispersion and vertical distribution during stationary anticyclonic conditions had their own specific features. The most typical cases were a uniform vertical profile up to 700 hPa (≈3 km) with a BC ratio of 8-20% among all the aerosol compounds. Very often there was no clear maximum within the lowest 3-km layer especially for the coarse and accumulation modes. The
320   urban areas with additional anthropogenic emissions were an exception where a maximum formed near the surface. This distribution differed from the other synoptic conditions, which resulted in a maximum BC concentration outside the emission areas at an altitude of 1.5 km (Kostrykin et al., 2021).

The decrease of radiation forcing (Chubarova et al., 2012) and a reduction of shortwave radiation (Pere et al, 2014) were
325   observed after wildfire aerosol emissions during summer 2010. Previously it was shown that the shortwave radiation is smaller on 70-84 W/m^2 in the diurnal averages (Pere et al., 2014). Our results confirmed the decrease in the downwelling surface short-wave radiation at the background as the result of the direct aerosol effects were up to -250 W/m^2 during the midday hours. However, numerous spots were observed, where the downwelling surface short-wave and long-wave radiation increased. The 2-m air temperature was higher in spite of considering the direct aerosol effects of the areas where the long-wave radiation
330   increased up to 20 W/m^2 and both BC coarse and accumulation mode exceeded values of 30 ppb. These hot-spots might coaligned with the BC impacts at certain locations, as the BC influence is known by its localizing effects with no clear directs

link between the pattern of forcing and pattern of temperature change (Modak and Bala, 2019). Overall, the direct radiative forcing and the consequent air temperature increase was estimated for BC regardless of the emission source (Ma et al., 2018; Zhuang et al., 2019; Kostrykin et al., 2021); however cooling effects also was detected (Ma et al., 2018). In combination with other aerosol types the effects on the radiative forcing also is variable (Kirkevag et. al, 1999). Hence, not all areas with air temperature increasing or decreasing are not directly connected with the prevailing influence of certain aerosol compound but a net effect including physical, chemical and meteorological effects are being experienced.

In the absence of BC measurements, ground-based monitoring network in Ukraine represents a challenge for the results validation. Nevertheless, it gives an overall picture of the BC distribution during unfavorable weather conditions and makes it possible for a provision of assessments in Ukraine on the quantify of BC influenced human health and local ecosystems in Ukraine as a whole. Moreover, the fact that the wildfire emissions can cause local the air temperature to increase amid elevated pollution levels is crucial for the understanding the consequences for vulnerable people. This is especially relevant during the heat wave events such as in August 2010, which is discussed in this study.

4 Conclusions

Employing the Enviro-HIRLAM online integrated modelling system, the patterns of the BC spatio-temporal distribution were estimated for selected elevated pollution period of August 2010 in Ukraine, which resulted from severe forest fires in the central part of Russia. For the first time, spatio-temporal BC content, distribution of its different particle sizes, and BC ratio among other aerosol compounds in the atmosphere with the emphasize on extremely hot period were analysed. Moreover, for the first time, the seamless online integrated meteorology - atmospheric composition modelling approach (with Enviro-HIRLAM model), compared to classical off-line approach (separate meteorology and atmospheric chemical transport modelling), was applied to geographical domain of Ukraine.

The highest BC content was observed in Ukraine in 2010 during two episodes 7-8 and 13-16 August because of air prevailing movement towards Ukraine from areas/ cells with burning forests. The stationary anticyclone and hence, favourable conditions with deep ~~nighttime~~night-time air temperature inversions caused constant emission distribution and large accumulative effect in the boundary level. BC was distributed over distances more than 2000 km from original emission sources. Over Ukraine, it reached 70-150 ppb for the accumulation mode and 50-80 ppb for the coarse mode. Anthropogenic emissions of BC Aitken mode prevailed over wildfires. Vertical transport was slower, and particles mainly dispersed in the lowest 3-km layer. However, the fingerprint of BC coarse and accumulation mode could be also detected in the middle troposphere (i.e., up to 660-630 hPa level for the coarse mode and up to 620-590 hPa for the accumulation mode). The temperature inversions at nights caused diurnal variability of the BC vertical distribution. Here, concentrations descended to the lower layers at night and ascend at daytime by weakening of downward air movement. For the near-surface level, the integral values over the

Eastern Ukraine, Azov Sea and Black Sea territories exceeded 800 and 150 ppb for the accumulation and coarse modes, respectively. ~~The features of the integral content distribution for the entire studied period and "tails" existence might be influenced also by the BC emissions from the local sources of fires that observed during these days in the eastern and north-eastern parts of Ukraine.~~ The highest BC-to-total aerosol content ratio was observed in the lower 200-m layer (up to 990 hPa) reaching 10-24% near the fires and over urban areas. The dominant aerosol compounds were organic carbon and sulfates. Hence, direct aerosol effects on radiative and temperature regimes in the region mostly were typical for these compounds: decreasing in downwelling surface short-wave radiation and decreasing of 2-m air temperature. In areas with high BC content representing by accumulation and coarse mode, downwelling long-wave radiation with direct aerosol effects was higher up to 20-25 W/m^2 during the midday hours. 2-m air temperature was 1-4°C higher in these regions with BC coarse mode exceeded 20-30 ppb.

The obtained results of the study are important and significant for improvement of quality of numerical weather prediction and for depicting the impacts of the extreme events with atmospheric chemical transport modelling. The findings are relevant for assessment studies of atmospheric pollutants impact on population and ecosystems health, for climate adaptation and socio-economical related studies, for optimization and establishing of air quality monitoring stations, decision- and policy making process, etc.

Overall, the study needs further development in two directions. First direction requires elaboration of ground-based BC measurements in Ukraine for modelling data validation and assessment the negative BC impact on human health and local ecosystems in Ukraine with future transition to mitigation measures and reduction strategy. Second direction should expand the analysis of direct and indirect aerosol effects using online-integrated modelling with separating the influences of different aerosol compounds.

Appendix A
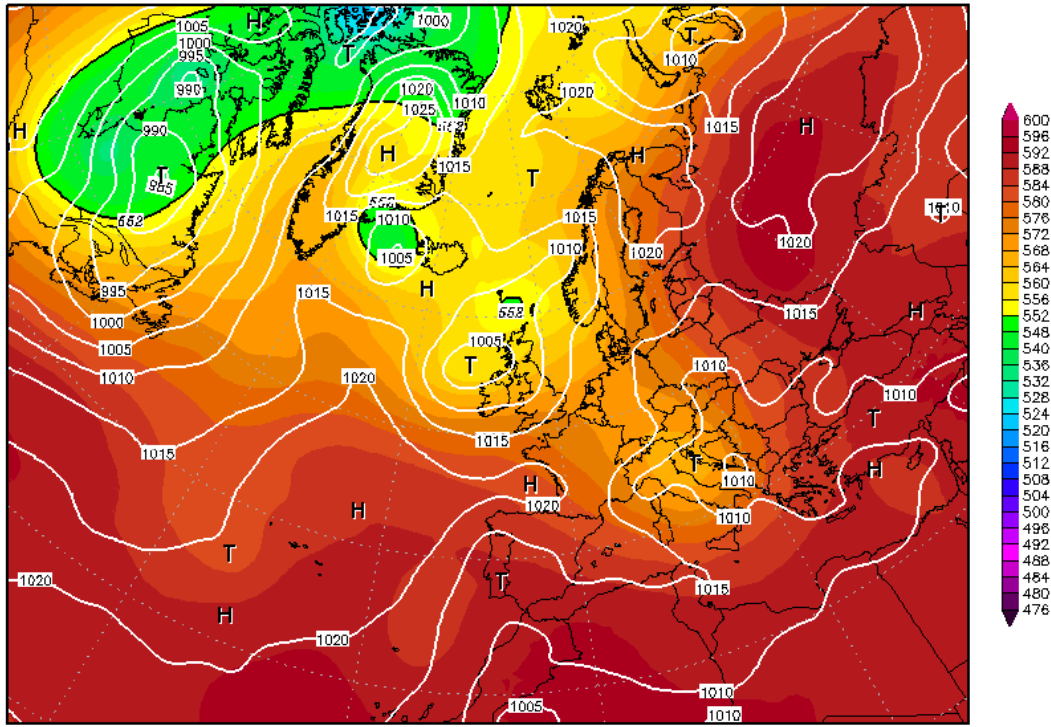
390 **Figure A1. 500 hPa geopotential over Europe on 6th August 2010 (source: www.wetterzentrale.de)**
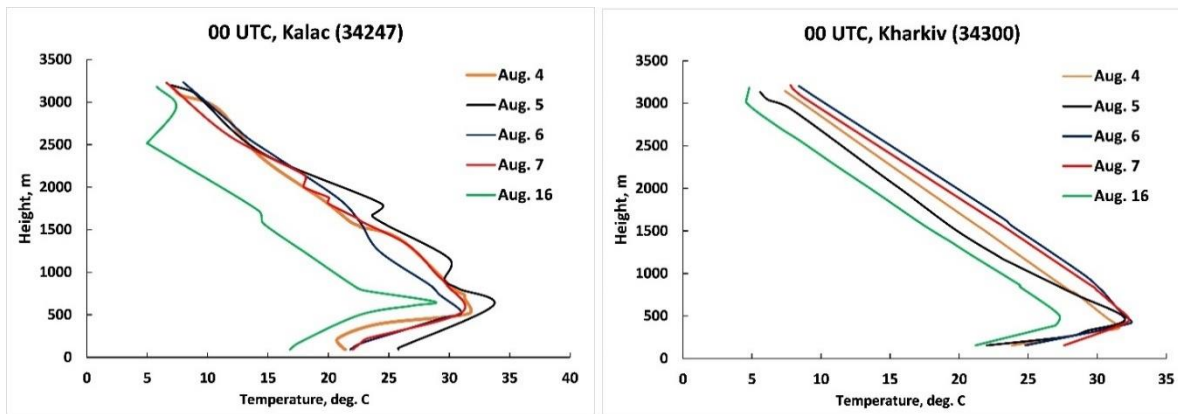
Figure A2: The air temperature vertical profiles from the vertical sounding stations Kalac and Kharkiv for selected dates (4-7 and 16 August 2010) with the deepest surface temperature inversions at nighttime (00 UTC).

395 *Code and data availability*. The code and data used in this study is available from the authors upon reasonable request.

Author Contributions. MS: Methodology, Investigation, Visualisation, Writing Original and Draft. LP: Investigation, Visualisation, Writing Original and Draft. SK: Conceptualization, Methodology, Supervision. AM: Conceptualization, Methodology, Supervision, Writing – Review and Editing. TP: Writing - Review and Editing. All authors provided comments
400 on manuscript.

Competing Interests. The authors declare that they have no conflict of interests.

Acknowledgements. The study is part of the Enviro-PEEX on ECMWF (Pan-Eurasian EXperiment (PEEX;
405 https://www.atm.helsinki.fi/peex) Modelling Platform research and development for online coupled integrated meteorology-chemistry-aerosols feedbacks and interactions in weather, climate and atmospheric composition multi-scale modelling) project (2018-2020).
The Enviro-HIRLAM model simulations were performed on the CSC (Center for Science Computing) Sisu HPC (Finland) during the Enviro-HIRLAM/ HARMONIE research training course at the Institute for Atmospheric and Earth System Research
410 (INAR), University of Helsinki (UHEL).
The financial support was provided by the grant within ENVRIplus project for Multi-domain Access to RI platforms "The Influence of Land cover changes On Atmospheric Boundary Layer and Regional Climate Characteristics" (2018).
The work partially has been performed under the Project HPC-EUROPA3 (INFRAIA-2016-1-730897), with the support of the EC Research Innovation Action under the H2020 Programme; in particular, the authors gratefully acknowledge the
415 computer resources and technical support provided by Center for Science Computing (CSC) HPC (Finland).
This study was carrying out by the financing of Ukrainian Hydrometeorological Institute within the framework of the State Emergency Service of Ukraine and National Academy of Sciences of Ukraine.

References

420 Amiro B.D., Todd J.B., Wotton B.M., Logan K.A., Flannigan M.D., Stocks B.J., Mason J.A., Martell D.L., and Hirsch K.G.: Direct carbon emissions from Canadian forest fires, 1959–1999., Can. J. For. Res., 31, 512–525, 2001.
Baklanov, A., Korsholm U.S., Nuterman R., Mahura A., Nielsen K.P., Sass B.H., Rasmussen A., Zakey A., Kaas E., Kurganskiy A., Sørensen B., and González-Aparicio I.: Enviro-HIRLAM online integrated meteorology–chemistry modelling system: strategy, methodology, developments and applications (v7.2)., Geosci. Model Dev., 10, 2971–2999, doi:
425 10.5194/gmd-10-2971-2017, 2017.
Barnaba F., Angelini F., Curci G., and Gobbi G.P.: An important fingerprint of wildfires on the European aerosol load., Atmos. Chem. Phys., 11, 10487–10501, doi: 10.5194/acp-11-10487-2011, 2011.

Bessagnet B., Menut L., Aymoz G., Chepfer H., and Vautard R.: Modeling dust emissions and transport within Europe: The Ukraine March 2007 Event., J. Geophys. Res.-Atmos., Vol. 113, D15202, doi: 10.1029/2007JD009541, 2008.

430 Bond T. C., Doherty S. J., Fahey D. W., Forster P. M., Berntsen T., DeAngelo B. J., Flanner M. G., Ghan S., Kärcher B., Koch D., Kinne S., Kondo Y., Quinn P. K., Sarofim M. C., Schultz M. G., Schulz M., Venkataraman C., Zhang H., Zhang S., Bellouin N., Guttikunda S. K., Hopke P. K., Jacobson M.Z., Kaiser J. W., Klimont Z., Lohmann U., Schwarz J. P., Shindell D., Storelvmo T., Warren S. G., and Zender C. S.: Bounding the role of black carbon in the climate system: A scientific assessment., J. Geophys. Res.-Atmos., 118, 5380–5552, doi:10.1002/jgrd.50171, 2013.

435 Castagna J., Senatore A., Bencardino M., D'Amore F., Sprovieri F., Pirrone N., and Mendicino G. Multiscale assessment of the impact on air quality of an intense wildfire season in southern Italy, Sci. Tot. Environ., 761, 143271, doi: 10.1016/j.scitotenv.2020.143271, 2021.

Christian T. J., Kleiss B., Yokelson R. J., Holzinger R., Crutzen P. J., Hao W. M., Saharjo B. H., and Ward D.E.: Comprehensive laboratory measurements of biomass-burning emissions: 1. Emissions from Indonesian, African, and other
440 fuels. Journal of Geophysical Research, 108(D23), 4719, doi: 10.1029/2003JD003704, 2003.

Chubarova N., Nezval, Ye., Sviridenkov I., Smirnov A., and Slutsker I.: Smoke aerosol and its radiative effects during extreme fire event over Central Russia in summer 2010., Atmos. Meas. Tech., 5, 557–568, doi:10.5194/amt-5-557-2012, 2012.

Eleftheriadis K., Vratolis S., and Nyeki S.: Aerosol black carbon in the European Arctic: Measurements at Zeppelin station, Ny-Ålesund, Svalbard from 1998–2007., Geophys. Res. Let., 36, L02809, doi: 10.1029/2008GL035741, 2009.

445 Forbes, M., Raison R.J., and Skjemstad J.O.: Formation, transformation and transport of black carbon (charcoal) in terrestrial and aquatic ecosystems., Sci Total Environ., 370(1), 190-206, doi: 10.1016/j.scitotenv.2006.06.007, 2000.

Galytska E., Danylevsky V., Hommel R., and Burrows J.P.: Increased aerosol content in the atmosphere over Ukraine during summer 2010., Atmos. Meas. Tech., 11, 2101–2118, doi: 10.5194/amt-11-2101-2018, 2018.

Galytska E., Danylevsky V., and Snizhko S.: Aerosols dynamics in the atmosphere over Eastern Europe by means of
450 AERONET according to weather conditions during summer 2010., Ukr. gìdrometeorol. ž., 17, 5-16, doi: 10.31481/uhmj.17.2016.01, 2016.

HIRLAM-5 Scientific Documentation, Per Unden, December 2002.

Hodzic A., Madronich S., Bohn B., Massie S., Menut L., and Wiedinmyer C.: Wildfire particulate matter in Europe during summer 2003: meso-scale modeling of smoke emissions, transport and radiative effects., Atmos. Chem. Phys., 7, 4043–4064,
455 doi:10.5194/acp-7-4043-2007, 2007.

Janssen N.A., Hoek G, Simic-Lawson M., Fischer P., van Bree L., ten Brink H., Keuken M., Atkinson R.W., Anderson H.R., Brunekreef B., and Cassee F.R.: Black carbon as an additional indicator of the adverse health effects of airborne particles compared to PM10 and PM2.5., Environ Health Perspect; 119(12), 1691-9, doi: 10.1289/ehp.1003369, 2011.

Jia, M., Evangeliou, S., Eckhardt, S., Huang, X., Gao, J., Ding, A., and Stohl, A. Black Carbon Emission Reduction Due to
460 COVID-19 Lockdown in China. Geophysical Research Letters, 48, e2021GL093243, doi: 10.1029/2021GL093243, 2021.

Jimenez J. L., Canagaratna M. R., Donahue N. M., Prevot A. S., H., Zhang Q., Kroll J. H., DeCarlo P. F., Allan J. D., Coe H., Ng N. L., Aiken A. C., Docherty K. S., Ulbrich I. M., Grieshop A. P., Robinson A. L., Duplissy J., Smith J. D., Wilson K. R., Lanz V. A., Hueglin C., Sun Y. L., Tian J., Laaksonen A., Raatikainen T., Rautiainen J., Vaattovaara P., Ehn M., Kulmala M., Tomlinson J. M., Collins D. R., Cubison M. J., Dunlea J., Huffman J. A., Onasch T. B., Alfarra M. R., Williams P. I., Bower K., Kondo Y., Schneider J., Drewnick F., Borrmann S., Weime, S., Demerjian K., Salcedo D., Cottrell L., Griffin R., Takami A., Miyoshi T., Hatakeyama S., Shimono A., Sun J. Y., Zhang Y. M., Dzepina K., Kimmel J. R., Sueper D., Jayne J. T., Herndon S. C., Trimborn A. M., Williams L. R., Wood E. C., Middlebrook A. M., Kolb C. E., Baltensperger U., and Worsnop D. R.: Evolution of Organic Aerosols in the Atmosphere. Science, 80, 1525–1529, doi: 10.1126/science.1180353, 2009

Kirkevåg A., Iversen T., and Dahlback A. On radiative effects of black carbon and sulphate aerosols. Atm. Env., 33, 2621-2635, doi: 10.1016/S1352-2310(98)00309-4, 1999.

Konovalov I.B., Beekmann M., Kuznetsova I.N., Yurova A., and Zvyagintsev A.M.: Atmospheric impacts of the 2010 Russian wildfires: integrating modelling and measurements of an extreme air pollution episode in the Moscow region. Atmos. Chem. Phys., 11, 10031–10056, doi: 10.5194/acp-11-10031-2011, 2011.

Konovalov I.B., Lvova D.A., Beekmann M., Jethva H., Mikhailov E.F., Paris J.-D., Belan B.D., Kozlov V.S., Ciais P., and Andreae M.O.: Estimation of black carbon emissions from Siberian fires using satellite observations of absorption and extinction optical depths. Atmos. Chem. Phys., 18, 14889–14924, doi: 10.5194/acp-18-14889-2018, 2018.

Kostrykin S., Revokatova A., Chernenkov A., Ginzburg V., Polumieva P., and Zelenova M. Black Carbon Emissions from the Siberian Fires 2019: Modelling of the Atmospheric Transport and Possible Impact on the Radiation Balance in the Arctic Region., Atmosphere, 12(7), 814, doi: 10.3390/atmos12070814, 2021.

Kurganskiy A., Nuterman R.B., Mahura A.G., Baklanov A.A., Sass B.H., and Kaas E. Enviro-HIRLAM black carbon modelling for Northern Europe and Arctic. Climate Change for Arctic Seas and Shipping: 3rd CRAICC-PEEX Workshop, 24-25 August 2015, Copenhagen, Denmark, Danish Meteorological Institute: programme and abstracts. P. 14, 2015.

Lee T., Sullivan A. P., Mack L., Jimenez J. L., Kreidenweis S. M., Onasch T. B., Worsnop D. R., Malm W., Wold C. E., Hao W. M., and Collett Jr, J. L.: Chemical Smoke Marker Emissions During Flaming and Smoldering Phases of Laboratory Open Burning of Wildland Fuels, Aerosol Science and Technology, 44:9, i-v, doi: 10.1080/02786826.2010.499884, 2010.

Lee H., Jeing S.-J., Kalashnikova O., Tosca M., Kim S.-W., and Kug J.-S. Characterization of Wildfire-Induced Aerosol Emissions From the Maritime Continent Peatland and Central African Dry Savannah with MISR and CALIPSO Aerosol Products. JGR Atmospheres, 123(6), 3116-3125, 2018.

Leino K., Riuttanen L., Nieminen T., Dal Maso M., Väänänen R., Pohja T., Keronen P., Järvi L., Aalto P.P., Virkkula A., Kerminen V.-M., Petäjä T. and Kulmala M. Biomass-buring smoke episodes in Finland from Eastern European wildfires, Boreal Environ Res. 19 B, 275-292, 2014.

Ma X., Liu H., Wang X., and Peng Z. Studies on the Climate Effects of Black Carbon Aerosols in China and Their Sensitivity to Particle Size and Optical Parameters. Advances in Meteorology, 2018, 9341026, doi: 10.1155/2018/9341026, 2018.

Magalhaes N.d., Evangelista H., Condom T., Rabatel A., and Ginot P. Amazonian Biomass Burning Enhances Tropical Andean Glaciers Melting. Sci Rep., 9, 16914, doi: 10.1038/s41598-019-53284-1, 2019

Matsui H., Hamilton D.S., and Mahowald N.M. Black carbon radiative effects highly sensitive to emitted particle size when resolving mixing-state diversity. Nat Commun., 9, 3446, doi: 10.1038/s41467-018-05635-1, 2018.

Modak, A., and Bala, G.: Efficacy of black carbon aerosols: the role of shortwave cloud feedback. Environ. Res. Lett., 14, 084029, doi: 10.1088/1748-9326/ab21e7. 2019

Nadtochii L.M., Savenets M.V., Bashtannik M.P., and Dvoretska I.V. The features of dust air pollution dynamics in certain Ukrainian cities. Ukr. geogr. z., 1, 43-50, doi: 10.15407/ugz2019.01.043, 2019.

Nightingale P. D., Malin G., Law C. S., Watson A. J., Liss P. S., Liddicoat M. I., Boutin J., and Upstill-Goddard R. C.: In situ evaluation of air-sea exchange parameterizations using novel conservative and volatile tracers, Global Biogeochem. Cycles, 14, 373–387, 2000

Nuterman R., Mahura A., Baklanov A., Kurganskiy A., Amstrup B., and Kaas E.: Enviro-HIRLAM Applicability for Black Carbon Studies in Arctic., Geophysical Research Abstracts, 17, EGU2015-1571, 2015.

O'Dell K., Hornbrook R.S., Permar W., Levin E., Garofalo L.A., Apel E.C., Blake N.J., Jarnot A., Pothier M.A., Farmer D.K., Lu Hu, Campos T., Ford B., Pierce J.R., and Fischer E.V. Hazardous Air Pollutants in Fresh and Aged Western US Wildfire Smoke and Implications for Long-Term Exposure, Environ. Sci. Technol., 54, 11838-11847, doi: 10.1021/acs.est.0c04497, 2020.

Pavese G., Calvello M., and Esposito F.: Black Carbon and Organic Components in the Atmosphere of Southern Italy: Comparing Emissions from Different Sources and Production Processes of Carbonaceous Particles., Aerosol and Air Quality Research, 12, 1146–1156, doi: 10.4209/aaqr.2011.12.0236, 2012.

RD 1991. RD 52-04. 186-89 Guidance on atmospheric air pollution control, USSR Hydrometeorological Service (in Russian).

Pere J.C., Bessagnet B., Mallet M., Waquet F., Chiapello I., Minvielle F., Pont V., and Menut L.: Direct radiative effect of the Russian wildfires and its impact on air temperature and atmospheric dynamics during August 2010. Atmos. Chem. Phys., 14, 1999–2013, doi: 10.5194/acp-14-1999-2014, 2014.

Popovicheva O.B., Engling G., Ku I.T., Timofeev M.A. and Shonija N.K.: Aerosol Emissions from Long-lasting Smoldering of Boreal Peatlands: Chemical Composition, Markers, and Microstructure. Aerosol Air Qual. Res., 19, 484-503, doi: 10.4209/aaqr.2018.08.0302, 2019.

Singh R.P., Kumar S., and Singh A.K. Elevated Black Carbon Concentrations and Atmospheric Pollution around Singrauli Coal-Fired Thermal Power Plants (India) Using Ground and Satellite Data. Int. J. Environ. Res. Public Health, 15(11), 2472, doi: 10.3390%2Fijerph15112472, 2018.

Sofiev M., Vankevich R., Lotjonen M., Prank M., Petukhov V., Ermakova T., Koskinen J., and Kukkonen J.: An operational system for the assimilation of the satellite information on wild-land fires for the needs of air quality modelling and forecasting, Atmos. Chem. Phys., 9, 6833–6847, doi: 10.5194/acp-9-6833-2009, 2009.

530 Stjern C.W., Samset B.H., Myhre G., Forster P.M., Hodnebrog Ø., Andrews T., Boucher O., Faluvegi G., Iversen T., Kasoar M., Kharin V., Kirkevag A., Lamarque J.-F., Olivie D., Richardson T., Shawki D., Shindell D., Smith C.J., Takemura T., and Voulgarakis A.: Rapid Adjustments Cause Weak Surface Temperature Response to Increased Black Carbon Concentrations. JGR Atmos., 122, 11462-11481, doi: 10.1002/2017JD027326, 2017.

WHO Report. Health effects of black carbon. 2012. http://www.euro.who.int/data/assets/pdf_file/0004/162535/e96541.pdf

Witte J.H., Douglass A.R., da Silva A., Torres O., Levy R., and Duncan B.N.: NASA A-Train and Terra observations of the 2010 Russian wildfires., Atmos. Chem. Phys., 11, 9287–9301, doi: 10.5194/acp-11-9287-2011, 2011.

Upper Air Soundings. Wyoming University: http://weather.uwyo.edu/upperair/sounding.html

535 Yang Yang, Hailong Wang, Steven J. Smith, Po-Lun Ma and Philip J. Rasch.: Source attribution of black carbon and its direct radiative forcing in China. Atmos. Chem. Phys., 17, 4319–4336, doi: 10.5194/acp-17-4319-2017, 2017.

Vadrevu K. P., Lasko K., Giglio L., and Justice C.: Vegetation fires, absorbing aerosols and smoke plume characteristics in diverse biomass burning regions of Asia. Environmental Research Letters, 10(10), 105003. doi: 10.1088/1748-9326/10/10/105003, 2015.

540 Virkkula A., Pohja T., Aalto P.P., Keronen P., Schobesberger S., Clements C.B., Petäjä T., Nikmo J. and Kulmala M. Airborne measurements of aerosols and carbon dioxide during a prescribed fire experiment at a boreal forest site, Boreal Environ. Res., 19 B, 153-181, 2014a.

Virkkula A., Levula J., Pohja T., Aalto P.P., Keronen P., Schobesberger S., Clements C.B., Pirjola L., Kieloaho A.-J., Kulmala L., Aaltonen H., Patokoski J., Pumpanen J., Rinne J., Ruuskanen T., Pihlatie M., Manninen H.E., Aaltonen V., Junninen H.,

545 Petäjä T., Backman J., Dal Maso M., Nieminen T., Olsson T., Grönholm T., Aalto J., Virtanen T.H., Kajos M., Kerminen V.-M., Schultz D.M., Kukkonen J., Sofiev M., De Leeuw G., Bäck J., Hari P. and Kulmala M. Prescribed burning of logging slash in the boreal forest in Finland: emissions and effects on meteorological quantities and soil properties, Atmos. Chem. Phys., 14, 4473-4502, doi: 10.5194/acp-14-4473-2014, 2014.

Wu Y., Anjeza A., Jianping H., Barry G., and Fred M. Intra-continental wildfire smoke transport and impact on local air quality

550 observed by ground-based and satellite remote sensing in New York City, Atmos. Environ. 187, 266-281, doi: 10.1016/j.atmosenv.2018.06.006, 2018.

Zhuang B.L., Chen H.M., Li S., Wang T.J., Liu J., Zhang L.J., Liu H.N., Xie M., Chen P.L., Li M.M., and Zhao M. The direct effects of black carbon aerosols from different source sectors in East Asia in summer. Clim Dyn 53, 5293–5310 (2019). https://doi.org/10.1007/s00382-019-04863-5

555 Yttri K. E., Aas W., Bjerke A., Cape J. N., Cavalli F., Ceburnis D., Dye C., Emblico L., Facchini M. C., Forster C., Hanssen J. E., Hansson H. C., Jennings S. G., Maenhaut W., Putaud J. P., and Torseth K.: Elemental and organic carbon in PM10: a one year measurement campaign within the European Monitoring and Evaluation Program EMEP, Atmos. Chem. Phys., 7, 5711-5725, doi: 10.5194/acp-7-5711-2007, 2007.